JOURNAL OF BACTERIOLOGY, Nov. 2009, p. 6539–6549 Vol. 191, No. 21
0021-9193/09/$12.00 doi:10.1128/JB.00414-09
Copyright © 2009, American Society for Microbiology. All Rights Reserved.

Molecular Analyses of a Three-Subunit Euryarchaeal Clamp Loader Complex from *Methanosarcina acetivorans*▽†

Yi-Hsing Chen,[1] Yuyen Lin,[1] Aya Yoshinaga,[2] Benazir Chhotani,[3] Jenna L. Lorenzini,[3] Alexander A. Crofts,[3] Shou Mei,[3] Roderick I. Mackie,[1,4] Yoshizumi Ishino,[2] and Isaac K. O. Cann[1,3,4]*

Department of Animal Sciences,[1] Department of Microbiology,[3] and Institute for Genomic Biology,[4] University of Illinois at Urbana-Champaign, Urbana, Illinois 61801, and Department of Genetic Resources Technology, Faculty of Agriculture, Kyushu University, Fukuoka-shi, Japan 812-8581[2]

Received 26 March 2009/Accepted 24 August 2009

Chromosomal DNA replication is dependent on processive DNA synthesis. Across the three domains of life and in certain viruses, a toroidal sliding clamp confers processivity to replicative DNA polymerases by encircling the DNA and engaging the polymerase in protein/protein interactions. Sliding clamps are ring-shaped; therefore, they have cognate clamp loaders that open and load them onto DNA. Here we use biochemical and mutational analyses to study the structure/function of the *Methanosarcina acetivorans* clamp loader or replication factor C (RFC) homolog. *M. acetivorans* RFC (RFC_{Ma}), which represents an intermediate between the common archaeal RFC and the eukaryotic RFC, comprises two different small subunits (RFCS1 and RFCS2) and a large subunit (RFCL). Size exclusion chromatography suggested that RFCS1 exists in oligomeric states depending on protein concentration, while RFCS2 exists as a monomer. Protein complexes of RFCS1/RFCS2 formed in solution; however, they failed to stimulate DNA synthesis by a cognate DNA polymerase in the presence of its clamp. Determination of the subunit composition and previous mutational analysis allowed the prediction of the spatial distribution of subunits in this new member of the clamp loader family. Three RFCS1 subunits are flanked by an RFCS2 and an RFCL. The spatial distribution is, therefore, reminiscent of the minimal *Escherichia coli* clamp loader that exists in space as three γ-subunits (motor) flanked by the δ′ (stator) and the δ (wrench) subunits. Mutational analysis, however, suggested that the similarity between the two clamp loaders does not translate into the complete conservation of the functions of individual subunits within the RFC_{Ma} complex.

Processive DNA synthesis is required to gain the speed necessary for the replication of large genomes as found in organisms across the three domains of life. Therefore, in each domain of life, molecular machines that ensure rapid DNA synthesis have evolved (17). At the center of the DNA synthesis machinery are the so-called replicative DNA polymerases and their processivity factors. Cells in all three domains of life, in addition to certain viruses, have evolved ring-shaped proteins, collectively called the processivity or sliding clamps, that repress the frequent dissociation of the DNA polymerase from the DNA template (17). The bacterial sliding clamp is known as the β-subunit, the eukaryotic functional homolog is called proliferating cell nuclear antigen (PCNA), and due to its similarity to the eukaryotic protein, the archaeal sliding clamp is also termed PCNA (4, 6, 12, 15). Among the viruses, the bacteriophage T4 clamp or gp45 has been well characterized (1). In each case, the clamp contains a cavity that is wide enough to allow it to encircle and slide freely along DNA (16, 18). However, since the clamp is a ring-shaped protein, it requires another protein to open and load it onto DNA. Thus, each clamp comes with its loader, also collectively known as the clamp loaders (2, 5, 29). Whereas the bacterial clamp loader is termed the γ-complex, the eukaryotic functional homolog is known as replication factor C or RFC (3, 19).

Cullmann and coworkers demonstrated that the heteropentameric RFC complex in eukaryotes is encoded by five different genes: four different genes coding for the RFC small subunit (RFCS) proteins and the last gene coding for the RFC large subunit (RFCL) proteins (9). In a subsequent analysis of clamp loaders in archaea, it was demonstrated that *Methanothermobacter thermautotrophicus* (20), *Sulfolobus solfataricus* (29), and *Pyrococcus furiosus* (5) each contain only one RFCS gene and one RFCL gene. The polypeptide sequences of the RFCS of the archaea exhibit very high homology to those of the four eukaryotic RFCS (6), suggesting the relatedness of the archaeal/eukaryotic RFC proteins. Interestingly, four protomers of the archaeal RFCS protein form a complex with one large subunit protein to act as the functional clamp loader (5, 29). Thus, similar to the eukaryotic RFC, the archaea appeared to have a pentameric RFC complex that harnesses energy, derived from ATP hydrolysis, to break open the ring-shaped clamp. The loader then loads the opened clamp onto a primer-template junction, thereby facilitating the interaction between the clamp and its cognate replicative DNA polymerase to ensure processive DNA synthesis (10, 13, 14).

We recently described a new form of clamp loader in the domain Archaea (7). Unlike all previously described clamp loaders from this domain, the *Methanosarcina acetivorans* RFC

* Corresponding author. Mailing address: Department of Animal Sciences, 1207 West Gregory Drive, University of Illinois at Urbana-Champaign, Urbana, IL 61801. Phone: (217) 333-2090. Fax: (217) 333-8286. E-mail: icann@illinois.edu.

† Supplemental material for this article may be found at http://jb.asm.org/.

▽ Published ahead of print on 28 August 2009.

TABLE 1. Oligonucleotides used in this study[a]

Experiment	Oligonucleotide	Nucleotide sequence
Truncations	MacRFCS2F	AAAACATATGGAATCAATGCAGGATCTCTGGACTCT
	MacRFCS2R	TTTTTCTCGAGTCAGGAGAATGTGGAAATCAATTTTTCG
	RFCS2Δ(85-110)F	GACTTTTTCGACCAGGGAATAGATATTTTTAAGGAAGTCGTT
	RFCS2Δ(85-110)R	AACGACTTCCTTAAAAATATCTATTCCCTGGTCGAAAAAGTC
	MacRFCLF	AAAAACATATGATGTCGGCAATCGAATGGGCTGAAAAAT
	RFCLΔ1(1-550)R	CTCGAGTTAGGTTTTCTGCTCTACAGATTCGGA
	RFCLΔ2(1-475)R	CTCGAGTTATTTGCCGGCAGAACCTTCCTTTTG
	RFCLΔ3(1-432)R	CTCGAGTTAATTCTTACCCTCTTCAAGAAGTTT
	RFCLΔ4(1-410)R	CTCGAGCTATGCACTTCCTGTAAGGTACATC
	RFCLΔ5(1-385)R	CTCGAGCTAGTCCTTCAGCATGCGGGAATAAAG
Mutations	RFCS1-K18A	GAGATCTGGATTGAAGCATACAGGCCTGTCAGG
	RFCS1-E82A	AGGGAAAACTTTACCGCACTTAATGCTTCCGAT
	RFCS1-E119A	ATCATTTTTCTTGATGCAGCCGATGCTCTAACA
	RFCS1-E136A	CTCCGCAGGACCATGGCACGGTTCAGCAGCAAC
	RFCS1-D205A	TACGTAGCTCAGGGAGCCATGCGAAAAGCTGTC
Primer extension	(M13 6205-6234)	ATTCGTAATCATGGTCATAGCTGTTTCCTG

[a] The experiments in which the oligonucleotides were used are indicated. The truncation oligonucleotides were used to truncate $RFCS2_{Ma}$ and $RFCL_{Ma}$. The mutation oligonucleotides were used to create site-directed mutations in the RFC boxes of the $RFCS1_{Ma}$ gene. The primer extension oligonucleotide was used in DNA synthesis with M13 ssDNA as the template. Restriction sites incorporated into the oligonucleotides are underlined.

(RFC_{Ma}) homolog has three different subunits instead of the usual two subunits, i.e., one small subunit and one large subunit (7). This new form of archaeal clamp loader may represent an intermediate stage in the evolution of the more complex RFC in eukaryotes from the less complex ones reported for archaea (7). In this report, we determined the subunit organization and propose the spatial distribution of subunits in the new form of the RFC complex. The predicted spatial distribution of the RFC_{Ma} is similar to the *Escherichia coli* minimal γ-complex, which is arranged as the "stator," "motor," and "wrench." Mutations in the predicted motor impaired the clamp loader's capacity to stimulate clamp-dependent DNA synthesis by a cognate DNA polymerase in *M. acetivorans* ($PolBI_{Ma}$). C-terminal truncations that removed putative clamp interacting motifs in the subunit occupying the wrench position failed to abolish the capacity of the loader to stimulate clamp-dependent DNA synthesis by the cognate DNA polymerase. Our results, therefore, suggested that although the *M. acetivorans* and the *E. coli* clamp loaders likely adopt similar subunit organization/spatial distribution, the functions of the individual subunits are unlikely to be fully conserved.

MATERIALS AND METHODS

Cloning, expression, and purification of the *M. acetivorans* clamp loader complex. The cloning, expression, and purification of $RFCS1_{Ma}$, $RFCS2_{Ma}$, $RFCL_{Ma}$, and RFC_{Ma} complex were described in our previous report (7).

Truncational analysis of the RFC_{Ma} complex. In a previous report (7), we showed that the *M. acetivorans* clamp loader complex (RFC_{Ma}) is composed of two small subunits ($RFCS1_{Ma}$ and $RFCS2_{Ma}$) and a large subunit ($RFCL_{Ma}$). The plasmid constructs for the expression of the individual subunits were designated pET28/*rfcl*, pET28/*rfcs1*, and pET28/*rfcs2* for N-terminal His_6-tagged RFCL, N-terminal His_6-tagged RFCS1, and N-terminal His_6-tagged RFCS2, respectively. To create an expression system for the RFC complex, RFCS1 and RFCS2 were placed in frame in the pACYCDuet vector (Novagen) to express the non-His_6-tagged and His_6-tagged proteins encoded by *rfcs1* and *rfcs2*, respectively. This expression vector was named pACYCDuet/*rfcs1*/*rfcs2*. The pET28a vector was previously modified through the substitution of the kanamycin resistance gene with that for ampicillin resistance (4). For the coexpression of the pACYCDuet/*rfcs1*/*rfcs2* construct, which contained a chloramphenicol resistance gene, and pET28a/*rfcl*, the recombinant *E. coli* culture was supplemented with ampicillin and chloramphenicol at 100 μg/ml and 50 μg/ml, respectively. RFCL and RFCS2 in the RFC_{Ma} complex, therefore, contained N-terminal His_6 tags.

To create C-terminal truncation derivatives of RFCL, a PCR method was used. All primers are shown in Table 1. To make five truncations of decreasing length from the C-terminal region of $RFCL_{Ma}$, PCR amplifications with a forward primer MacRFCLF in combination with five different reverse primers—RFCLΔ1(1-550)R, RFCLΔ2(1-475)R, RFCLΔ3(1-432)R, RFCLΔ4(1-410)R, and RFCLΔ5(1-385)R—were carried out. The template was the gene coding for wild-type $RFCL_{Ma}$, and the RFC complexes derived from the truncated proteins were designated RFC-LΔ1, RFC-LΔ2, RFC-LΔ3, RFC-LΔ4, and RFC-LΔ5, respectively. Each truncation targeted a region predicted to form a loop in the protein structure (Predictprotein [http://www.ebi.ac.uk/~rost/predictprotein/predictprotein.html]). Each PCR product was initially cloned into a pGEM-T Easy vector (Promega) and sequenced to confirm the integrity of the sequence. The RFCL truncated genes were then individually cloned into pET28a as described for the wild-type RFCL gene (7).

Deletion of a 26-amino-acid insertion sequence in $RFC2_{Ma}$. A 26-amino-acid insertion sequence in $RFCS2_{Ma}$ was deleted by a PCR overlap method described in our previous report (30). The PCR primers that were used to delete the insertion sequence, as well as fuse the flanking sequences, were MacRFCS2F/RFCS2Δ(85-110)R and RFCS2Δ(85-110)F/MacRFCS2R (Table 1).

Point mutations in five RFC boxes in $RFCS1_{Ma}$. The oligonucleotides that were used to create point mutations in RFC boxes II, IV, V, VI, and VIII of RFCS1 are listed in Table 1 as RFCS1-K18A, RFCS1-E82A, RFCS1-E119A, RFCS1-E136A, and RFCS1-D205A, respectively. The method used was as described by the manufacturer for the QuikChange site-directed mutagenesis kit (Stratagene). All DNA inserts were sequenced (W. M. Keck Center for Comparative and Functional Genomics, University of Illinois at Urbana-Champaign) to confirm the presence of the desired mutations.

Estimation of subunit organization by size exclusion chromatography. To estimate the subunit organization of individual $RFCS_{Ma}$ subunits and also their mixtures, the purified proteins were dialyzed against buffer A containing 50 mM Tris-HCl (pH 8.0) and 300 mM NaCl. Different concentrations of each protein in a 100-μl total volume were then loaded onto a Superdex 200 HR 10/30 gel filtration column (GE Healthcare) already equilibrated with the same buffer, and the chromatography was developed at 4°C. For the mixtures of $RFCS1_{Ma}$ and $RFCS2_{Ma}$, various amounts of the individual proteins were mixed and dialyzed against buffer A for 1 h before the gel filtration analysis. The chromatography was developed with the same buffer at a flow rate of 0.5 ml/min, and fractions of 0.5 ml were collected and aliquots were analyzed on 8% sodium dodecyl sulfate-polyacrylamide gel electrophoresis (SDS-PAGE) gels. The gel filtration column was calibrated by running a set of protein standards (thyroglobulin, 669 kDa; ferritin, 440 kDa; aldolase, 158 kDa; catalase, 58 kDa; ovalbumin, 43 kDa; and RNase A, 13.7 kDa) under the same conditions.

Stoichiometry of RFC_{Ma} complex and spatial arrangement. The stoichiometric ratio of RFCS1, RFCS2, and RFCL in the RFC_{Ma} complex was determined through a densitometric method as in our previous report on *Pyrococcus furiosus* RFC (RFC_{Pf}) complex (5). The RFC_{Ma} complex was resolved through SDS-PAGE, and after being stained with Coomassie brilliant blue followed by destaining, the gels were scanned with a densitometer. Each band was then quantified from a calibration curve obtained by using each purified subunit at different concentrations to obtain a relationship between protein band intensity and the amount of protein loaded for the electrophoretic analysis.

CD scan. The wild-type RFC_{Ma} complex and its mutants were subjected to circular dichroism (CD) scans to determine if individual mutations impacted the secondary structural elements of the protein complex. The method used was the same as described in our previous report (23). However, in this case, we used 0.5 μg/μl of each protein in a buffer composed of 50 mM Tris-HCl (pH 8.0), 200 mM NaCl, 5 mM $MgCl_2$, 10% glycerol, and 1 mM dithiothreitol. Triplicate data sets were collected per protein under investigation, and all data were normalized against readings obtained from buffer without protein.

Cloning, expression, and purification of $PCNA_{Ma}$ and $PolBI_{Ma}$. The methods for the production of *M. acetivorans* PCNA or the sliding clamp and the *M. acetivorans* DNA $PolBI_{Ma}$ were as described in our previous report (7).

Primer extension analysis. To prepare the substrate per primer extension reaction, 500 ng of bacteriophage M13mp18 single-stranded DNA (ssDNA) template and 1 pmol 5′-^{32}P-end-labeled primer (Table 1), complementary to positions 6205 to 6234 of the template, were annealed by heating to 95°C for 5 min and cooling slowly to room temperature in a buffer composed of 20 mM Tris-HCl (pH 8.8), 100 mM NaCl, 5 mM $MgCl_2$, and 2 mM β-mercaptoethanol. Where multiple reactions were carried out, the annealing reaction mixture was scaled up by the number of reactions required. Thus, each primer extension reaction (total volume of 20 μl) contained 1 pmol of the end-labeled primer annealed to 500 ng of template, 250 μM of each deoxynucleoside triphosphate, and 20 mM ATP in the buffer used for the annealing reaction. To initiate primer extension, the cognate DNA polymerase, $PolBI_{Ma}$, was added to the reaction mixture at 0.24 μM. Where the effects of accessory factors were investigated, they were added at 77.5 nM of RFC_{Ma} complex or its mutants, and 0.3 μM of $PCNA_{Ma}$ (based on the PCNA trimer) per reaction. In the case of the $RFCS_{Ma}$, the amounts of RFCS added ranged from 1.5 to 15 μM/reaction. The primer extension reaction was carried out at 37°C for 5 min and terminated with 6 μl of stop solution (98% formamide, 1 mM EDTA, 0.1% xylene cyanol, 0.1% bromophenol blue). After being heated to 95°C for 5 min, the samples were resolved on a 1% alkali agarose gel and visualized by autoradiography.

Amino acid sequence alignments. The amino acid sequence alignments were carried out using ClustalW2 (http://www.ebi.ac.uk/Tools/clustalw2/index.html), and the shading was manually carried out.

RESULTS

Oligomerization state of *M. acetivorans* clamp loader small subunits. We successfully expressed both $RFCS1_{Ma}$ and $RFCS2_{Ma}$ as N-terminal His_6-tagged proteins. After purification, however, the His_6 tag was removed from each protein by protease (thrombin) digestion. In a previous analysis of an archaeal RFCS (*Pyrococcus furiosus* homolog), we reported that the protein oligomerized in solution (5). Subsequent analysis by electron microscopy (25) and X-ray crystallography (32) of the archaeal RFCS detected proteins existing as mostly homohexamers, although at different pH values, $RFCS_{Pf}$ also existed as homopentamers and homotetramers. These oligomerization states were not observed for either of the two $RFCS_{Ma}$, although $RFCS1_{Ma}$ was estimated to exist as a dimer (7). Thus, in the present experiment, we sought to examine the oligomerization state of the two $RFCS_{Ma}$ proteins as their concentrations were varied. $RFCS1_{Ma}$ and $RFCS2_{Ma}$ have estimated molecular masses of 37.9 and 38.3 kDa, respectively. The elution volumes in our gel filtration analysis, however, suggested that the oligomerization state of $RFCS1_{Ma}$ was concentration dependent. As protein concentration increased, we observed a change from monomers to homodimers, homotrimers, and finally homotetramers at 40 μg/μl (Fig. 1A). On the other hand, increasing concentrations of $RFCS2_{Ma}$ to 40 μg/μl did not lead to oligomerization of this protein, which was estimated to exist as a monomer in solution (Fig. 1B). It is of interest that we observed differential staining of $RFCS1_{Ma}$ and $RFCS2_{Ma}$ in our SDS-PAGE analysis (Fig. 1A and B). It is our assumption that this is due to differences in the amino acid contents, especially arginine, and to a lesser extent amino acids such as histidine, lysine, and the aromatic residues, such as tryptophan, tyrosine, and phenylalanine (8, 11). In the case of $RFCL_{Ma}$, it consistently eluted in the void volume, as reported earlier (7), suggesting a protein of a very large molecular mass (results not shown).

In the absence of RFCS1, RFCS2 eluted at a peak elution volume around 14.8 ml (Fig. 1B). However, when the two purified proteins were dialyzed together and analyzed by size exclusion chromatography, $RFCS2_{Ma}$ eluted earlier with $RFCS1_{Ma}$, suggesting an interaction between the two proteins (Fig. 1C). $RFCS1_{Ma}$ alone at 2 μg/μl was estimated as a monomer (Fig. 1A), and at a concentration of 20 μg/μl, $RFCS2_{Ma}$ also eluted as a monomer (Fig. 1B). However, when we mixed $RFCS1_{Ma}$ and $RFCS2_{Ma}$ at 2 μg/μl and 20 μg/μl, respectively, we observed two peaks representing dimers (82.0 ± 0.9 kDa) and monomers (37.4 ± 0.1 kDa). This suggested that the two proteins interacted and that the dimers were likely heterodimers of the two proteins. $RFCS1_{Ma}$ at 5 μg/μl eluted as a dimer (Fig. 1A). However, when mixed with $RFCS2_{Ma}$ at 20 μg/μl, there were two peaks that were estimated as 104.1 ± 8.0 kDa and 38.2 ± 0.6 kDa. This may suggest a heterotrimer of $RFCS1_{Ma}$/$RFCS2_{Ma}$ and monomers of the individual proteins, respectively. By mixing $RFCS1_{Ma}$ and $RFCS2_{Ma}$ at concentrations of 20/2, 20/5, and 20/20 μg/μl, respectively, we also observed two peaks. The elution volume of the first peak suggested either a trimer or tetramers of the RFCS proteins (117 to 127 kDa), and the second peak suggested monomers (36.2 to 38.2 kDa).

Subunit organization and spatial distribution of the RFC_{Ma} complex. The stoichiometric ratio of RFCS1, RFCS2, and RFCL in the functional RFC complex was determined through a densitometric method as described in our previous report for the *Pyrococcus furiosus* RFC complex (5). The concentrations of the RFC subunits shown in Fig. 2A were calculated to be 71.0 pmol, 25.6 pmol, and 22.4 pmol for RFCS1, RFCS2, and RFCL, respectively (Fig. 2B). The results, therefore, suggested that $RFCS1_{Ma}$, $RFCS2_{Ma}$, and $RFCL_{Ma}$ form a stable complex with a stoichiometric ratio of 3:1:1. Note that the differential staining of $RFCS1_{Ma}$ and $RFCS2_{Ma}$ should not impact our estimated stoichiometry, since the individual proteins were used to generate their individual prediction equation that related intensity to the amount of protein loaded on the gel. Based on the stoichiometric information and our previous data on mutagenesis in the individual subunits (7) within the RFC complex, we predicted the spatial distribution in Fig. 2C, and this is further discussed later.

Truncational analysis of the large subunit of RFC_{Ma} complex. The spatial arrangement of the subunits in the RFC_{Ma} complex suggested above is similar to that of the *E. coli* minimal clamp loader, which also has a 3:1:1 ratio and is made up of three γ subunits (motor) flanked by the stator (δ′) and the wrench (δ) (10). The wrench interacts with the *E. coli* sliding clamp and on its own is able to open the clamp through this

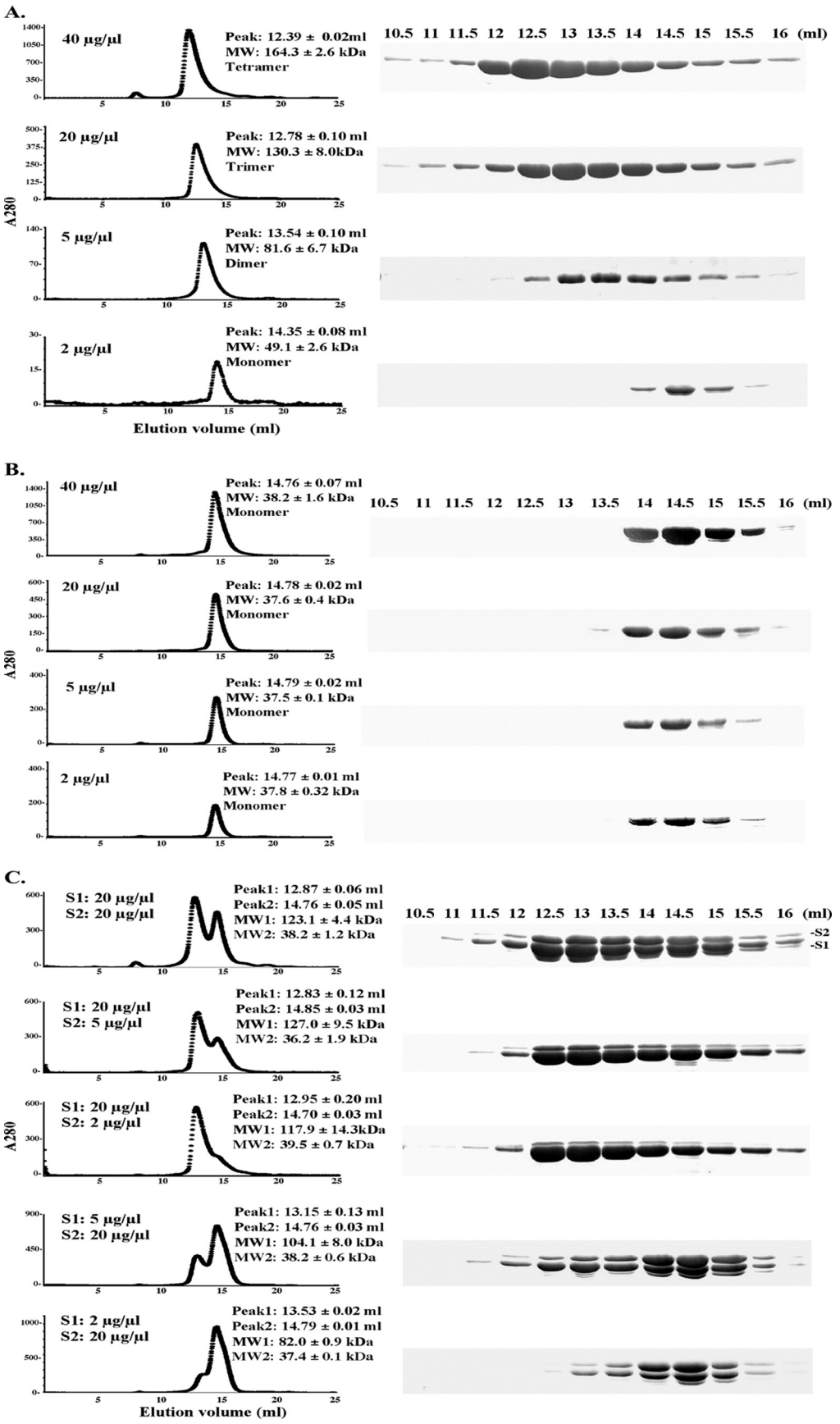
A.
40 μg/μl
Peak: 12.39 ± 0.02ml
MW: 164.3 ± 2.6 kDa
Tetramer
20 μg/μl
Peak: 12.78 ± 0.10 ml
MW: 130.3 ± 8.0kDa
Trimer
5 μg/μl
Peak: 13.54 ± 0.10 ml
MW: 81.6 ± 6.7 kDa
Dimer
2 μg/μl
Peak: 14.35 ± 0.08 ml
MW: 49.1 ± 2.6 kDa
Monomer
A280
Elution volume (ml)
10.5 11 11.5 12 12.5 13 13.5 14 14.5 15 15.5 16 (ml)
B.
40 μg/μl
Peak: 14.76 ± 0.07 ml
MW: 38.2 ± 1.6 kDa
Monomer
20 μg/μl
Peak: 14.78 ± 0.02 ml
MW: 37.6 ± 0.4 kDa
Monomer
5 μg/μl
Peak: 14.79 ± 0.02 ml
MW: 37.5 ± 0.1 kDa
Monomer
2 μg/μl
Peak: 14.77 ± 0.01 ml
MW: 37.8 ± 0.32 kDa
Monomer
A280
10.5 11 11.5 12 12.5 13 13.5 14 14.5 15 15.5 16 (ml)
C.
S1: 20 μg/μl
S2: 20 μg/μl
Peak1: 12.87 ± 0.06 ml
Peak2: 14.76 ± 0.05 ml
MW1: 123.1 ± 4.4 kDa
MW2: 38.2 ± 1.2 kDa
S1: 20 μg/μl
S2: 5 μg/μl
Peak1: 12.83 ± 0.12 ml
Peak2: 14.85 ± 0.03 ml
MW1: 127.0 ± 9.5 kDa
MW2: 36.2 ± 1.9 kDa
S1: 20 μg/μl
S2: 2 μg/μl
Peak1: 12.95 ± 0.20 ml
Peak2: 14.70 ± 0.03 ml
MW1: 117.9 ± 14.3kDa
MW2: 39.5 ± 0.7 kDa
S1: 5 μg/μl
S2: 20 μg/μl
Peak1: 13.15 ± 0.13 ml
Peak2: 14.76 ± 0.03 ml
MW1: 104.1 ± 8.0 kDa
MW2: 38.2 ± 0.6 kDa
S1: 2 μg/μl
S2: 20 μg/μl
Peak1: 13.53 ± 0.02 ml
Peak2: 14.79 ± 0.01 ml
MW1: 82.0 ± 0.9 kDa
MW2: 37.4 ± 0.1 kDa
A280
Elution volume (ml)
10.5 11 11.5 12 12.5 13 13.5 14 14.5 15 15.5 16 (ml)
-S2
-S1

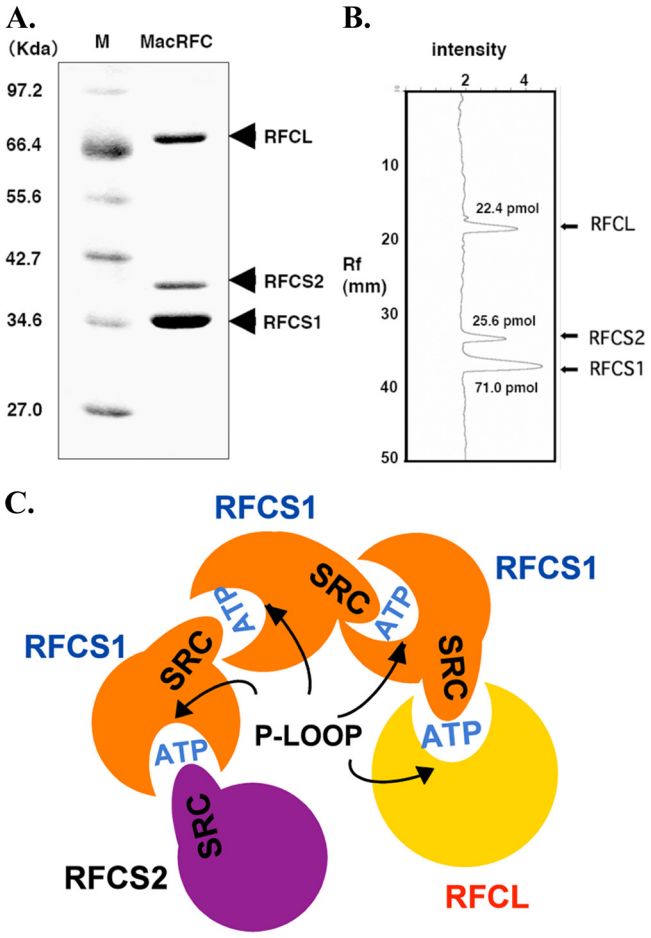

FIG. 2. Determination of the stoichiometry of the RFC_{Ma} complex. (A) RFC_{Ma} (MacRFC) complex resolved through SDS-PAGE. (B) Densitometer scan of the gel generates a relationship between protein band intensity and the amount of protein loaded for the electrophoretic analysis. Rf, relative to front value. (C) Schematic representation of the predicted spatial distribution of the RFC_{Ma} complex, which is similar to that of the *E. coli* clamp loader, based on stoichiometric ratio and mutational analysis at individual ATPase sites in the RFC complex (17). RFC proteins are members of AAA^+ ATPases, and the ATPase sites are at the interface between two adjacent subunits. One subunit provides a Walker A motif and the other an arginine finger from its SRC motif to form a competent ATPase site. Note that in the model, an ATPase site is missing at the interface of the large subunit and RFCS2, since RFCS2 has a Walker A motif but RFCL lacks an SRC motif.

interaction (17). In Fig. 3A, the *M. acetivorans* RFCL, which occupies the position of the wrench in the *E. coli* clamp loader, has two putative PCNA interacting protein (PIP) boxes at the C-terminal region: PIP box 1 (QKTLFDF; amino acids 596 to 602) and PIP box 2 (QKTLNMGF; amino acids 488 to 495) in Fig. 3C. The PIP boxes are known to mediate interactions with sliding clamps or PCNA (34). We, therefore, carried out a series of truncations from the C terminus of $RFCL_{Ma}$ to determine whether the removal of elements in the C-terminal region, especially the PIP boxes, will affect clamp stimulation of DNA synthesis in the presence of the RFC_{Ma} complex. As shown in Fig. 3B, we successfully produced four of the five RFC complex proteins that contained truncated derivatives of $RFCL_{Ma}$. The last RFCL-truncated derivative, RFC-LΔ5 (which has the last 222 amino acids removed), could not be obtained (results not shown). An examination of the *E. coli* cells expressing this RFC complex showed that the truncated RFCL failed to express. The first and second truncation mutants, RFC-LΔ1 and RFC-LΔ2, removed PIP box 1 and both PIP box 1/PIP box 2, respectively (7). However, as shown in Fig. 3Di and ii, lanes 4, both mutant clamp loader complexes stimulated $PCNA_{Ma}$-dependent DNA synthesis by $PolBI_{Ma}$, suggesting that both RFC-LΔ1 and RFC-LΔ2 are capable of loading the sliding clamp. The results were, therefore, similar to those of the primer extension in the presence of the wild-type RFC complex (Fig. 3D, lanes 6). The subsequent deletions that removed 175 amino acids (RFC-LΔ3; Fig. 3C) and 197 amino acids (RFC-LΔ4; Fig. 3C) from the C terminus, respectively, also did not lead to the failure to load $PCNA_{Ma}$ (Fig. 3Diii and iv, lanes 4).

Mutations in some conserved RFC boxes of $RFCS1_{Ma}$ impair RFC_{Ma}-dependent $PCNA_{Ma}$ stimulation of DNA synthesis by $PolBI_{Ma}$. Eight conserved motifs, referred to as RFC box I to box VIII, were previously identified in RFC proteins (9). The conservation of seven of these RFC boxes (box II to box VIII) was later confirmed in archaeal RFCS proteins (6). In the present work, we hypothesized that other than RFC box III (Walker A motif or P-loop) and box VII (SRC motif), which have been shown to be critical for ATPase activity and, therefore, the clamp loading function of RFC proteins including the RFC_{Ma} complex (7), the other RFC boxes, especially those in the putative motor domain, are likely to play important roles in the function of this new clamp loader. To test our hypothesis, we made a single mutation at a conserved residue in each of RFC box II [$RFCS1(K18A)_{Ma}$], box IV [$RFCS1(E82A)_{Ma}$], box V [$RFCS1(E119A)_{Ma}$], box VI (D136A), and box VIII (D205A) (Fig. 4). Each mutant RFCS1 was used in reconstituting an RFC_{Ma} complex that harbored that single mutation. To ensure that each mutation did not lead to gross changes in the secondary structural elements, each RFC complex containing the respective mutation was highly purified (results not shown) and subjected to CD scan. As shown in Fig. 5A, except for the RFC complex protein containing $RFCS1_{Ma}$-E119A (mutation in box V), the other mutant RFC complex proteins exhibited CD spectra that were similar to that of the wild-type RFC_{Ma} complex. It should be noted, however, that the clamp

FIG. 1. Gel filtration analysis of RFC_{Ma} subunits and mixtures of $RFCS1_{Ma}$ and $RFCS2_{Ma}$. The native molecular masses of RFC_{Ma} subunits were estimated by gel filtration on a Superdex 200 HR 10/30 column fitted to a high-performance liquid chromatography apparatus. Indicated amounts of highly purified individual $RFCS_{Ma}$ proteins and their mixtures were dialyzed and then injected into the column to estimate native molecular masses. The results are presented as $RFCS1_{Ma}$ (A), $RFCS2_{Ma}$ (B), and a mixture of $RFCS1_{Ma}$ and $RFCS2_{Ma}$ (C). The elution volumes are indicated, and fractions were analyzed by SDS-PAGE to visualize the proteins. $RFCS1_{Ma}$ tends to degrade with time. The band that appears below $RFCS1_{Ma}$ is known to be $RFCS1_{Ma}$ processed at the N terminus (7). MW, molecular weight.

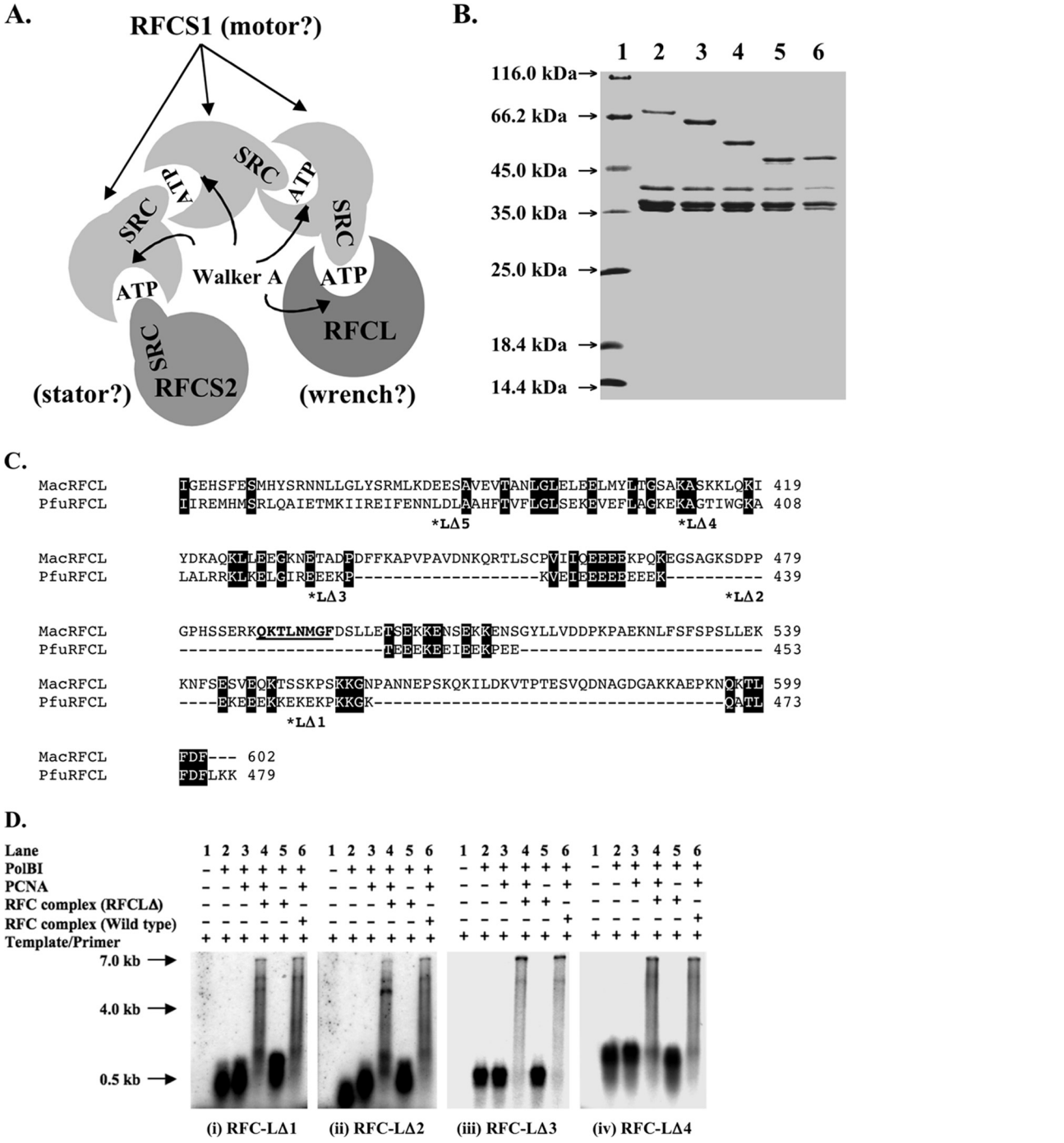

FIG. 3. Hypothetical functions of the *M. acetivorans* clamp loader subunits. (A) The proposed model of the RFC_{Ma} subunit arrangement is similar to that of the *E. coli* minimal clamp loader, the γ-complex. The $RFCS2_{Ma}$, $RFCS1_{Ma}$, and $RFCL_{Ma}$ subunits occupy the positions of the stator, the motor, and the wrench, respectively, in the *E. coli* protein complex. (B) SDS-PAGE of the purified recombinant wild-type RFC_{Ma} complex and RFC_{Ma} complex proteins containing truncated $RFCL_{Ma}$. Lane 1, protein molecular mass markers (Fermentas); lane 2, wild-type RFC_{Ma} complex; lane 3, *M. acetivorans* RFC-LΔ1 complex; lane 4, *M. acetivorans* RFC-LΔ2 complex; lane 5, *M. acetivorans* RFC-LΔ3 complex; lane 6, *M. acetivorans* RFC-LΔ4 complex. (C) Alignment of the C-terminal region of $RFCL_{Pf}$ (PfuRFCL) and $RFCL_{Ma}$ (MacRFCL) showing the single and double PIP boxes in $RFCL_{Pf}$ and $RFCL_{Ma}$, respectively. In addition, the points of the truncations in $RFCL_{Ma}$ are denoted by asterisks and the different truncations shown as LΔX, where X represents 1, 2, 3, 4, or 5. The basic amino acid sequence in $RFCL_{Pf}$ (KEKEKPKKGK) and the mostly acidic amino acid sequence (EEEKEEIEE KPEEEKEEE) are shown. (D) Effects of RFC_{Ma} complex proteins containing truncated $RFCL_{Ma}$ on the primer extension capacity of $PolBI_{Ma}$ in the presence of $PCNA_{Ma}$. Primer extensions were compared as follows: lanes 1, template alone or negative control; lanes 2, template/$PolBI_{Ma}$; lanes 3, template/$PolBI_{Ma}$/$PCNA_{Ma}$; lanes 4, template/$PolBI_{Ma}$/$PCNA_{Ma}$/*M. acetivorans* RFC-LΔ mutants; lanes 5, template/$PolBI_{Ma}$/*M. acetivorans* RFC-LΔ (i.e., lanes 4 without $PCNA_{Ma}$); lanes 6, template/$PolBI_{Ma}$/$PCNA_{Ma}$/RFC_{Ma} wild type or positive control. The substrate for DNA synthesis was 0.5 μg of singly primed M13mp18 ssDNA in DNA polymerase reaction buffer (described in Materials and Methods). The reaction mixtures were incubated at 37°C for 5 min, and the products were resolved by 1% alkali agarose gel electrophoresis and visualized by autoradiography. Note that the RFC_{Ma} complex in the absence of PCNA has no effect on DNA synthesis by $PolBI_{Ma}$ (7).

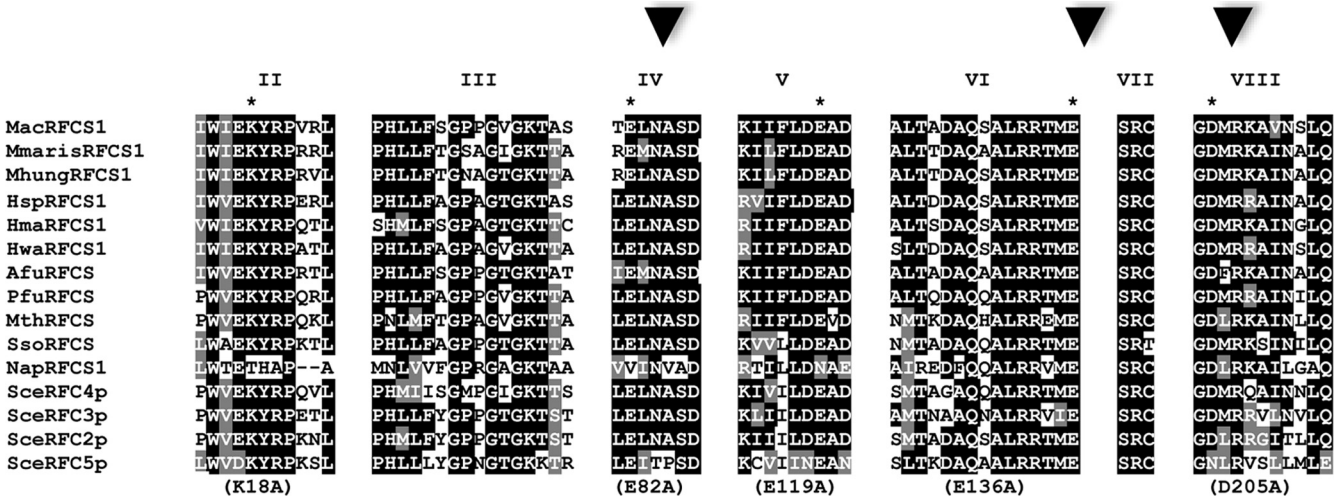

FIG. 4. An alignment showing the conserved RFC boxes in RFCS in both archaea and eukaryote *Saccharomyces cerevisiae*. The GenBank accession numbers of the proteins are as follows: *Methanosarcina acetivorans* C2A RFCS1 (MacRFCS1), NP_615630; *Methanoculleus marisnigri* JR1 RFCS1 (MmarisRFCS1), YP_001047161; *Methanospirillum hungatei* JF-1 RFCS1 (MhungRFCS1), YP_502463; *Halobacterium* sp. strain NRC-1 RFCS1 (HspRFCS1), NP_280914; *Haloarcula marismortui* RFCS1 (HmaRFCS1), YP_137064; *Haloquadratum walsbyi* DSM RFCS1 (HwaRFCS1), YP_659332; *Archaeoglobus fulgidus* RFCS (AfuRFCS), NP_070884; *Pyrococcus furiosus* RFCS (PfuRFCS), NP_577822; *Methanothermobacter thermautotrophicus* RFCS (MthRFCS), NP_275384; *Sulfolobus solfataricus* RFCS (SsoRFCS), NP_342275; *Natronomonas pharaonis* RFCS1 (NapRFCS1), YP_326110; *Saccharomyces cerevisiae* RFCS4 (SceRFC4p), EDV10522; *S. cerevisiae* RFCS3 (SceRFC3p), NP_014109; *S. cerevisiae* RFCS2 (SceRFC2p), EDV12808; and *S. cerevisiae* RFCS5 (SceRFC5p), NP_009644. Organisms with subunits designated -S1 are archaeal organisms with two RFCS (refer to the legend to Fig. 6). Conserved and similar amino acid residues are shaded black and gray, respectively. The asterisks denote the residue mutated to alanine in a given RFC box. Mutations in the RFC boxes with arrowheads impaired RFC-dependent $PCNA_{Ma}$ stimulation of DNA synthesis by $PolBI_{Ma}$.

loader complex containing E82A (RFC box IV) also showed some deviation from the wild type. The results, thus, suggested that at least three of the mutations (K18A, E136A, and D205A) did not severely impact the secondary structural elements of the RFC_{Ma} complex. Using primer extension analysis, we observed that three of the mutations made in $RFCS1_{Ma}$ (putative motor) impaired the capacity of the mutant RFC complex to stimulate $PCNA_{Ma}$-dependent DNA synthesis by $PolBI_{Ma}$. These were the mutations in RFC box IV (E82A; Fig. 5Bii, lane 4), box VI (E136A; Fig. 5Biv, lane 4), and box VIII (D205; Fig. 5Bv, lane 4). While the mutation in RFC box II (K18A) did not appear to impair the capacity of the RFC_{Ma} complex to stimulate $PCNA_{Ma}$-dependent DNA synthesis by $PolBI_{Ma}$ (Fig. 5Bi, lane 4), we observed a decreased aptitude in the case of the clamp loader complex containing the E119A mutation (Fig. 5Biii, lane 4). Each protein was compared with the wild-type RFC_{Ma} complex, serving as a positive control (Fig. 5B, lanes 6).

The insertion sequence downstream of RFC box IV in $RFCS2_{Ma}$ is not required for clamp loading. In archaeal RFCS2 polypeptides deposited in GenBank (http://www.ncbi.nlm.nih.gov/), an insertion sequence occurs downstream of RFC box IV (9) as shown in Fig. 6A. In the order *Methanosarcinales*, the insertion sequence comprises 26 amino acids that are highly conserved (7). To determine if the insertion sequence plays a role in PCNA loading, a PCR approach was used to delete the insertion sequence from $RFCS2_{Ma}$, and an RFC complex containing the mutant $RFCS2_{Ma}$, instead of the wild-type protein, was highly purified (results not shown). The RFC_{Ma} complex containing the mutant RFCS2 (RFCS2Δ; Fig. 6B) was tested for its capacity to enhance primer extension by $PolBI_{Ma}$ in the presence of the cognate clamp or $PCNA_{Ma}$. As shown in Fig. 6B, lane 4, deletion of the insertion sequence in $RFCS2_{Ma}$, although it appears to have slightly impaired the capacity of the protein complex to stimulate $PCNA_{Ma}$-dependent DNA synthesis by $PolBI_{Ma}$, did not abolish the clamp loading activity. We look forward to characterizing the mutant in detail. It should also be noted that the deleted sequence may play a role in a different function, for example, in interactions with other proteins.

The $RFCS1_{Ma}$/$RFCS2_{Ma}$ complex is unable to stimulate $PCNA_{Ma}$-dependent DNA synthesis by $PolBI_{Ma}$. As demonstrated above, we detected interactions that suggested heterodimer formation and either heterotrimer or heterotetramer formation between $RFCS1_{Ma}$ and $RFCS2_{Ma}$ (Fig. 1C). The peak fraction from each subunit organization was used, in a primer extension analysis, to determine whether the complex of the *M. acetivorans* RFCS can stimulate $PCNA_{Ma}$-dependent DNA synthesis by $PolBI_{Ma}$. In each case, the complex of the small subunits rather inhibited DNA synthesis, suggesting that they cannot load PCNA (see Fig. S1 in the supplemental material). The results were, therefore, similar to our previous findings that the individual subunits of RFC inhibit DNA synthesis by $PolBI_{Ma}$ (7). A similar finding showing the inhibition of a cognate DNA polymerase (Pol δ) by human RFCS has been reported elsewhere (28).

DISCUSSION

Pyrococcus furiosus RFCS (5, 27) and *Archaeoglobus fulgidus* RFCS (32) were shown to exist in oligomeric forms. Unlike the usual archaeal clamp loader proteins, the RFC_{Ma} complex has

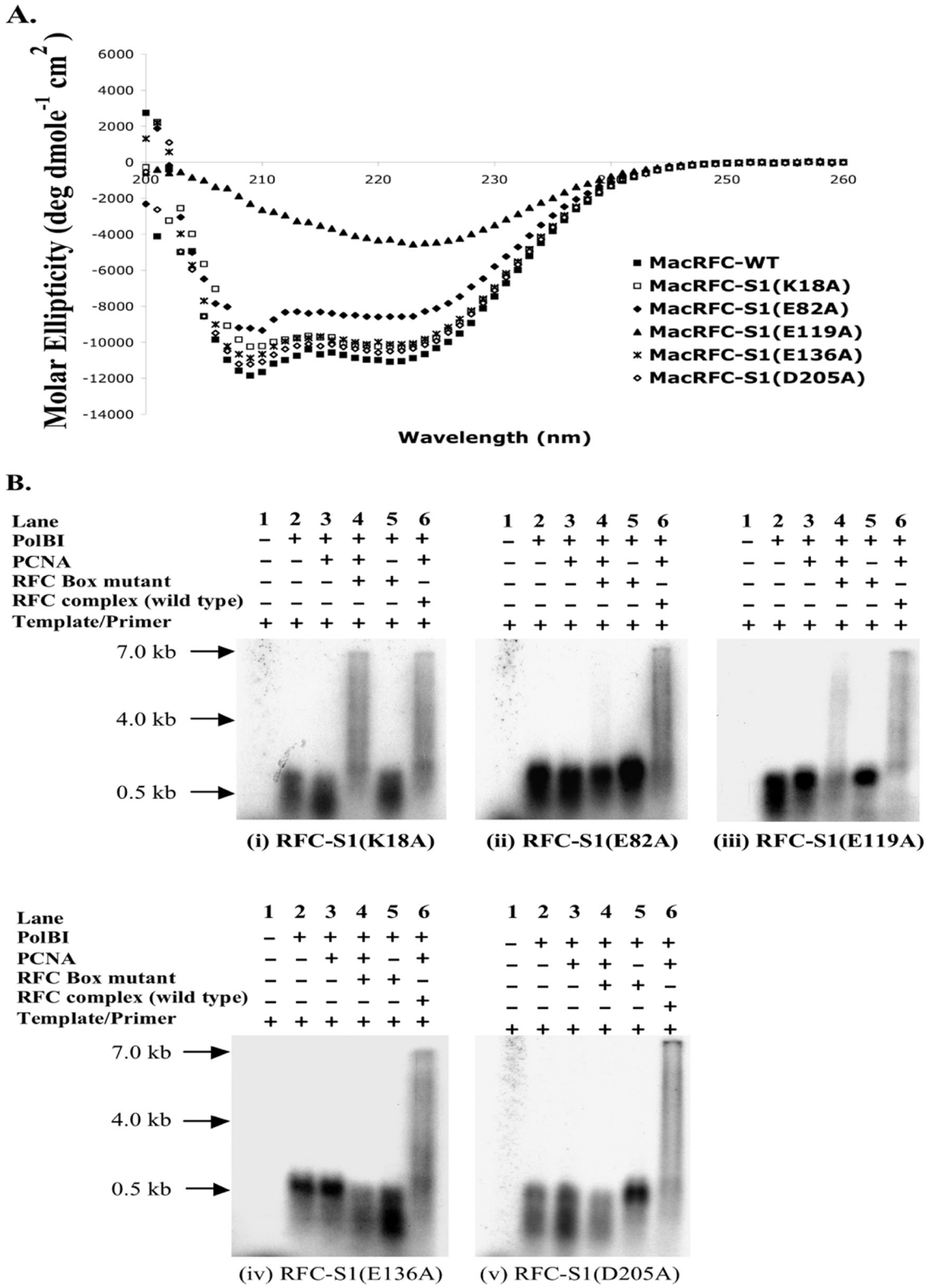

FIG. 5. Mutational analysis within different conserved RFC boxes in the motor domain of the RFC_{Ma} complex. (A) The highly purified RFC_{Ma} complex and its RFC box mutant derivatives were subjected to CD scans. The CD spectra of each protein from 200 nm to 260 nm were collected in triplicate and normalized against readings from buffer without protein. The samples analyzed were the wild-type RFC_{Ma} complex (MacRFC-WT); $RFCS1(K18A)_{Ma}$ complex [MacRFC-S1(K18A)], mutation in RFC box II; $RFCS1(E82A)_{Ma}$ complex [MacRFC-S1(E82A)], mutation in RFC box IV; $RFCS1(E119A)_{Ma}$ complex [MacRFC-S1(E119A)], mutation in RFC box V; $RFCS1(E136A)_{Ma}$ complex [MacRFC-S1(E136A)], mutation in RFC box VI; and $RFCS1(D205A)_{Ma}$ complex [MacRFC-S1(D205A)], mutation in RFC box VIII. (B) Effect of individual mutations in the RFC boxes on the capacity of the RFC_{Ma} complex to stimulate primer extension of $PolBI_{Ma}$ in the presence of $PCNA_{Ma}$. Lane 1, template

two small subunits (7). In the present report, we show that RFCS1$_{Ma}$ can exist as monomers and also as oligomers, ranging from homodimers to homotetramers, and that the oligomerization state is dependent on the protein concentration. In contrast, RFCS2$_{Ma}$ only exists as monomers in solution, irrespective of the protein concentration. The amino acid sequence alignment of RFCS1$_{Ma}$ and RFCS2$_{Ma}$ with other archaeal RFCS proteins (results not shown) suggests that RFCS1$_{Ma}$ is more similar to the known archaeal RFCS proteins. Thus, the RFCS1$_{Ma}$ polypeptide exhibits 59%, 50%, 49%, and 63% identities to the RFCS proteins found, respectively, in *P. furiosus*, *Methanothermobacter thermautotrophicus*, *Sulfolobus solfataricus*, and *A. fulgidus* (5, 20, 29, 31). RFCS2$_{Ma}$, on the other hand shows 29 to 38% identities to these proteins. A mixture of RFCS1$_{Ma}$/RFCS2$_{Ma}$ coeluted during size exclusion chromatography (Fig. 1C), suggesting that the two proteins interacted in solution. Although the protein complexes are likely to contain both RFCS1$_{Ma}$ and RFCS2$_{Ma}$, they may also contain protein complexes made up of only RFCS1, since this protein can undergo self-oligomerization. Samples from the peak fractions of the oligomerized RFCS1$_{Ma}$/RFCS2$_{Ma}$ failed to stimulate PCNA$_{Ma}$-dependent DNA synthesis by PolBI$_{Ma}$, suggesting that the complexes of the RFCS$_{Ma}$ proteins are incapable of loading the sliding clamp.

The stoichiometry and spatial distribution of RFC$_{Ma}$ subunits in the functional clamp loader were also determined in this report. In our model, three RFCS1$_{Ma}$ protomers are flanked by an RFCS2$_{Ma}$ on one side and by an RFCL$_{Ma}$ on the other side (Fig. 2C). This arrangement can be inferred from the estimated stoichiometry and our previous mutational analysis that showed that a critical mutation in the Walker A motif of RFCS2 has no effect on clamp-loading activity (7). The observation implied that the Walker A motif of RFCS2$_{Ma}$ does not participate in ATP binding/hydrolysis. RFC proteins are AAA$^+$ ATPases (17), and the ATPase sites are formed by a Walker A motif (RFC box III) from one subunit and an arginine finger (R in the SRC motif or RFC box VII) from an adjacent subunit. In the spatial arrangement shown in Fig. 2C, the Walker A (P-loop) of RFCS2 does not participate in ATP binding, and therefore, it does not influence ATP hydrolysis. A mutation in the Walker A motif of RFCL$_{Ma}$ (one ATPase site) also did not impair clamp-loading activity by RFCL$_{Ma}$. On the other hand, mutations in either the SRC or Walker A motif of RFCS1$_{Ma}$, which should affect three ATP binding sites according to our predicted spatial distribution (Fig. 2C), abolished clamp-loading activity (7). Both ATP binding and hydrolysis are required for the conformational changes that lead to clamp loading (17), and our previous mutational data (7) therefore support our proposed spatial distribution. The spatial arrangement of the RFC$_{Ma}$ complex is, therefore, likely to be similar to the *E. coli* minimal clamp loader (10, 17).

Subunits of the *E. coli* γ-complex are capable of binding to the sliding clamp or β-subunit. The δ wrench exhibits the strongest interaction with the β-clamp, and by itself, it can load and unload the clamp (17, 21, 33). The γ_3, on the other hand, binds less tightly and is also less competent in unloading the β-clamp (22). The δ′ is known as the stator or the stationary part of the γ-complex upon which the other subunits move, and its arginine finger together with the P-loop or Walker A motif of the adjacent γ-protomer forms the first ATPase site (site 1) in the γ-complex (35), as also shown in Fig. 3A for RFC$_{Ma}$. In archaea, RFCL is known to interact with the sliding clamp or PCNA (4). The C-terminal region of RFCL$_{Ma}$, which occupies the position analogous to the *E. coli* wrench, harbors two putative PIP boxes (Fig. 3C), although previously described RFCL proteins in archaea have only one PIP box (4, 6). This interaction between PCNA and the PIP box, by analogy, is similar to the interaction between the wrench (clamp-opening subunit) and the sliding clamp. Each of our four deletions from the C terminus of RFCL$_{Ma}$ (Fig. 3B), however, failed to abolish the stimulation of PCNA-dependent enhancement of DNA synthesis by PolBI$_{Ma}$. Thus, it is likely that although the subunit organization and spatial distribution of the RFC$_{Ma}$ complex are similar to the minimal *E. coli* clamp loader, interaction through the PIP boxes in the large subunit (wrench position) is not required for clamp loading. Note that in *Methanosarcina acetivorans*, instead of an octapeptide PIP box, several PCNA-interacting proteins have rather a conserved heptapeptide PIP box (7; I. K. O. Cann et al., unpublished data).

It was demonstrated previously that the RFCL$_{Pf}$ contains 10 amino acids that form a basic cluster (motif) immediately upstream of the PIP box, and upstream of the basic cluster is another amino acid cluster mainly composed of acidic residues (26). These clusters are present in RFCL$_{Ma}$ (Fig. 3C). However, unlike the RFCL$_{Pf}$ and its homologs in other thermophilic archaea, such as *Aeropyrum pernix*, *Methanocaldococcus jannaschii*, and *M. thermautotrophicus*, the RFCL$_{Ma}$ has >30 amino acids separating the basic residues from the most C-terminal PIP box. Furthermore, the acidic-residue-rich (glutamic acid-rich) region is split by several amino acids in the case of RFCL$_{Ma}$ (Fig. 3C). The basic amino acid cluster, and not the acidic cluster, was shown to be required for the formation of a ternary complex of RFC$_{Pf}$/PCNA$_{Pf}$/DNA (26). Furthermore, although the PIP box in RFCL$_{Pf}$ was shown to bind tightly to the sliding clamp (24), in support of our data presented here, the PIP box was shown to be nonessential for the RFC-dependent enhancement of DNA synthesis by PolBI$_{Pf}$ in the presence of its cognate PCNA (24).

The analysis of the polypeptides constituting the eukaryotic RFC proteins clearly showed that they contain conserved motifs that were designated RFC boxes (9). These motifs were also conserved in archaeal RFC proteins (6, 7). Although RFC box 1 is unique to the eukaryotic RFCL, box II to box VIII are common to all RFCS proteins (6). The functions of RFC box III (Walker A motif) and RFC box VII (SRC motif) in the

alone; lane 2, template/PolBI$_{Ma}$; lane 3, template/PolBI$_{Ma}$/PCNA$_{Ma}$; lane 4, template/PolBI$_{Ma}$/PCNA$_{Ma}$/RFC$_{Ma}$ mutant complex; lane 5, lane 4 without PCNA$_{Ma}$; lane 6, template/PolBI$_{Ma}$/PCNA$_{Ma}$/RFC$_{Ma}$ wild type (positive control). The primer extension reaction mixtures were incubated at 37°C for 5 min, and the products were analyzed by 1% alkali agarose gel electrophoresis, followed by visualization through autoradiography. The results in panels i, ii, iii, iv, and v represent the RFC complex containing the RFCS1$_{Ma}$ box II, IV, V, VI, and VIII mutants, respectively.

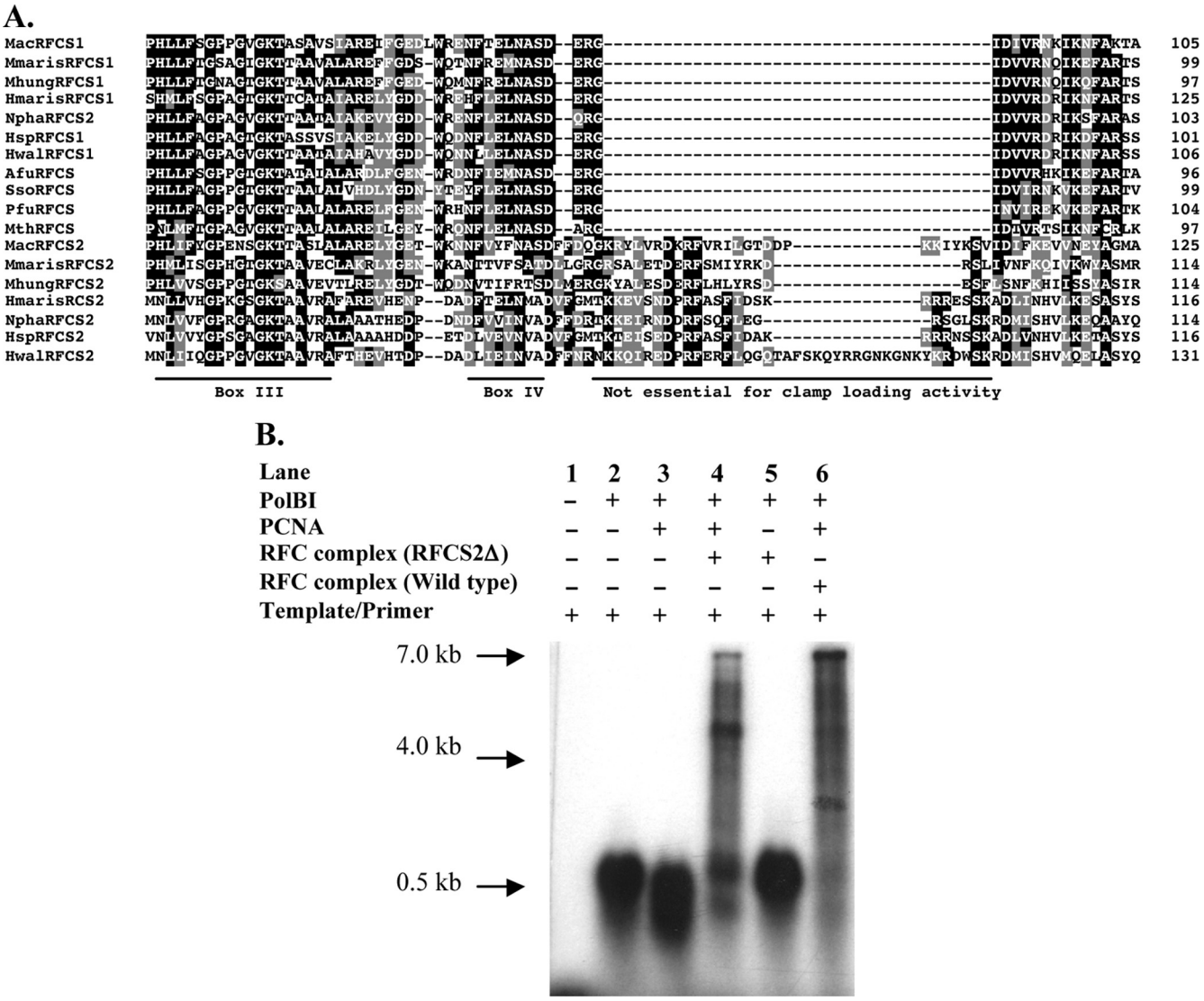

FIG. 6. Effect of an insertion sequence in RFCS2$_{Ma}$ on PCNA$_{Ma}$-dependent DNA synthesis by PolBI$_{Ma}$. (A) Alignment depicting insertion sequences downstream of RFC box IV regions in RFCS2$_{Ma}$ and its homologs. The GenBank accession numbers of the proteins are as follows: *M. acetivorans* RFCS1 (MacRFCS1), NP_615630; *M. marisnigri* RFCS1 (MmarisRFCS1), YP_001047161; *M. hungatei* JF-1 RFCS1 (MhungRFCS1), YP_502463; *H. marismortui* RFCS1 (HmarisRFCS1), YP_137064; *N. pharaonis* RFCS1 (NphaRFCS1), YP_326110; *Halobacterium* sp. strain NRC-1 RFCS1 (HspRFCS1), NP_280914; *Haloquadratum walsbyi* DSM RFCS1 (HwalRFCS1), intein-containing, YP_659332; *A. fulgidus* RFCS (AfuRFCS), NP_070884; *S. solfataricus* RFCS (SsoRFCS), NP_342275; RFCS$_{Pf}$ (PfuRFCS), intein-containing, NP_577822; *M. thermautotrophicus* RFCS (MthRFCS), NP_275384; *M. acetivorans* RFCS2 (MacRFCS2), NP_615114; *M. marisnigri* RFCS2 (MmarisRFCS2), YP_001047146; *M. hungatei* JF-1 RFCS2 (MhungRFCS2), YP_502304; *H. marismortui* RFCS2 (HmarisRFCS2), YP_136998; *N. pharaonis* RFCS2 (NphaRFCS2), YP_326194; *Halobacterium* sp. strain NRC-1 RFCS2 (HspRFCS2), NP_280882; and *H. walsbyi* DSM RFCS2 (HwalRFCS2), YP_659090. Conserved and similar amino acid residues are black and gray, respectively. (B) Deletion of the insertion sequence in RFCS2$_{Ma}$ does not abolish the stimulation of DNA synthesis by the RFC$_{Ma}$ complex. Lane 1, template alone; lane 2, template/PolBI$_{Ma}$; lane 3, template/PolBI$_{Ma}$/PCNA$_{Ma}$; lane 4, template/PolBI$_{Ma}$/PCNA$_{Ma}$/RFC$_{Ma}$-RFCS2Δ complex; lane 5, lane 4 without PCNA$_{Ma}$; lane 6, template/PolBI$_{Ma}$/PCNA$_{Ma}$/RFC$_{Ma}$ wild type or positive control. The substrate for DNA synthesis was 0.5 μg of singly primed M13mp18 ssDNA in DNA polymerase reaction buffer. The reaction mixtures were incubated at 37°C for 5 min, the products were resolved by 1% alkali agarose gel electrophoresis, and signals were detected by autoradiography.

archaeal and eukaryotic proteins are well described since the two motifs fold to form the competent ATPase sites in the protein complex (3, 10). To our knowledge, the other RFC boxes have not been investigated for their contribution to the structure/function of an RFC complex. Thus, as a first step to understanding the importance of these motifs in the RFC$_{Ma}$ complex, we targeted conserved amino acids in the RFC boxes of RFCS1$_{Ma}$, which may serve as the motor in the clamp loader complex. The importance of RFCS1 was demonstrated in our previous report, where we showed that single mutations in a conserved lysine in the Walker A motif or the conserved arginine in the SRC motif in this subunit abolished RFC-dependent stimulation of PolBI$_{Ma}$ during DNA synthesis in the presence of PCNA. This observation suggested failure to load the clamp by the mutant RFC$_{Ma}$ complex (7). Interestingly, E119A slightly stimulated PCNA$_{Ma}$-dependent DNA synthesis by

$PolBI_{Ma}$. Whereas the mutation in RFC box II (K18A) did not appear to impact the clamp loader's capacity to stimulate PCNA-dependent DNA synthesis by $PolBI_{Ma}$ (Fig. 5B), the three remaining mutations completely abolished the capacity of the clamp loader to stimulate DNA synthesis by the cognate DNA polymerase in the presence of its clamp.

Hence, we demonstrate that, in addition to box III (Walker A motif) and box VII (SRC motif), the integrity of three other RFC boxes in the motor domain of the RFC_{Ma} complex is critical to the clamp-loading reaction. These data agree with our recent biophysical analysis that captures the loading of a dye-labeled clamp to a dye-labeled primer/template junction of a DNA template (C. Liu et al., unpublished data). Similar assays have been used to observe clamp loading in other systems (36).

The RFC_{Ma} complex represents the only biochemically characterized member of this new family of archaeal/eukaryotic RFC. This type of RFC is expected in most haloarchaea, since the available genome sequences of representatives, such as *Halobacterium* sp. strain NRC-1, *Haloarcula marismortui*, *Haloquadratum walsbyi*, and *Natronomonas pharaonis*, have the three subunits in their genomes. In addition, several mesophilic methanogens, such as *Methanospirillum hungatei* and *Methanoculleus marisnigri*, have the genes encoding orthologs of RFC_{Ma} subunits. It is anticipated that the subunit organization, spatial distribution, and mutational data described for RFC_{Ma} will be applicable to the clamp loader complex proteins in these organisms and other relatives yet to be described.

ACKNOWLEDGMENTS

We thank William Metcalf (University of Illinois) for providing *M. acetivorans* genomic DNA and Taekjip Ha and Chen Liu (University of Illinois) for insightful discussions.

This research was supported by a National Science Foundation grant, MCB-0238451, to I.K.O.C. Also, Y.-H.C. and Y.L. were supported by National Science Foundation grant MCB-0238451.

REFERENCES

1. **Benkovic, S. J., A. M. Valentine, and F. Salinas.** 2001. Replisome-mediated DNA replication. Annu. Rev. Biochem. **70:**181–208.
2. **Bowman, G. D., E. R. Goedken, S. L. Kazmirski, M. O'Donnell, and J. Kuriyan.** 2005. DNA polymerase clamp loaders and DNA recognition. FEBS Lett. **579:**863–867.
3. **Bowman, G. D., M. O'Donnell, and J. Kuriyan.** 2004. Structural analysis of a eukaryotic sliding DNA clamp-clamp loader complex. Nature **429:**724–730.
4. **Cann, I. K., S. Ishino, I. Hayashi, K. Komori, H. Toh, K. Morikawa, and Y. Ishino.** 1999. Functional interactions of a homolog of proliferating cell nuclear antigen with DNA polymerases in *Archaea*. J. Bacteriol. **181:**6591–6599.
5. **Cann, I. K., S. Ishino, M. Yuasa, H. Daiyasu, H. Toh, and Y. Ishino.** 2001. Biochemical analysis of replication factor C from the hyperthermophilic archaeon *Pyrococcus furiosus*. J. Bacteriol. **183:**2614–2623.
6. **Cann, I. K., and Y. Ishino.** 1999. Archaeal DNA replication: identifying the pieces to solve a puzzle. Genetics **152:**1249–1267.
7. **Chen, Y. H., S. A. Kocherginskaya, Y. Lin, B. Sriratana, A. M. Lagunas, J. B. Robbins, R. I. Mackie, and I. K. Cann.** 2005. Biochemical and mutational analyses of a unique clamp loader complex in the archaeon *Methanosarcina acetivorans*. J. Biol. Chem. **280:**41852–41863.
8. **Compton, S. J., and C. G. Jones.** 1985. Mechanism of dye response and interference in the Bradford protein assay. Anal. Biochem. **151:**369–374.
9. **Cullmann, G., K. Fien, R. Kobayashi, and B. Stillman.** 1995. Characterization of the five replication factor C genes of *Saccharomyces cerevisiae*. Mol. Cell. Biol. **15:**4661–4671.
10. **Davey, M. J., D. Jeruzalmi, J. Kuriyan, and M. O'Donnell.** 2002. Motors and switches: AAA+ machines within the replisome. Nat. Rev. Mol. Cell Biol. **3:**826–835.
11. **De Moreno, M. R., J. F. Smith, and R. V. Smith.** 1986. Mechanism studies of Coomassie blue and silver staining of proteins. J. Pharm. Sci. **75:**907–911.
12. **Dionne, I., N. P. Robinson, A. T. McGeoch, V. L. Marsh, A. Reddish, and S. D. Bell.** 2003. DNA replication in the hyperthermophilic archaeon *Sulfolobus solfataricus*. Biochem. Soc. Trans. **31:**674–676.
13. **Gomes, X. V., and P. M. Burgers.** 2001. ATP utilization by yeast replication factor C. I. ATP-mediated interaction with DNA and with proliferating cell nuclear antigen. J. Biol. Chem. **276:**34768–34775.
14. **Gomes, X. V., S. L. Schmidt, and P. M. Burgers.** 2001. ATP utilization by yeast replication factor C. II. Multiple stepwise ATP binding events are required to load proliferating cell nuclear antigen onto primed DNA. J. Biol. Chem. **276:**34776–34783.
15. **Grabowski, B., and Z. Kelman.** 2003. Archaeal DNA replication: eukaryal proteins in a bacterial context. Annu. Rev. Microbiol. **57:**487–516.
16. **Gulbis, J. M., Z. Kelman, J. Hurwitz, M. O'Donnell, and J. Kuriyan.** 1996. Structure of the C-terminal region of p21(WAF1/CIP1) complexed with human PCNA. Cell **87:**297–306.
17. **Indiani, C., and M. O'Donnell.** 2006. The replication clamp-loading machine at work in the three domains of life. Nat. Rev. Mol. Cell Biol. **7:**751–761.
18. **Jeruzalmi, D., M. O'Donnell, and J. Kuriyan.** 2002. Clamp loaders and sliding clamps. Curr. Opin. Struct. Biol. **12:**217–224.
19. **Jeruzalmi, D., M. O'Donnell, and J. Kuriyan.** 2001. Crystal structure of the processivity clamp loader gamma (γ) complex of *E. coli* DNA polymerase III. Cell **106:**429–441.
20. **Kelman, Z., and J. Hurwitz.** 2000. A unique organization of the protein subunits of the DNA polymerase clamp loader in the archaeon *Methanobacterium thermoautotrophicum* deltaH. J. Biol. Chem. **275:**7327–7336.
21. **Leu, F. P., M. M. Hingorani, J. Turner, and M. O'Donnell.** 2000. The delta subunit of DNA polymerase III holoenzyme serves as a sliding clamp unloader in *Escherichia coli*. J. Biol. Chem. **275:**34609–34618.
22. **Leu, F. P., and M. O'Donnell.** 2001. Interplay of clamp loader subunits in opening the beta sliding clamp of *Escherichia coli* DNA polymerase III holoenzyme. J. Biol. Chem. **276:**47185–47194.
23. **Lin, Y., C. E. Guzman, M. C. McKinney, S. K. Nair, T. Ha, and I. K. Cann.** 2006. *Methanosarcina acetivorans* flap endonuclease 1 activity is inhibited by a cognate single-stranded-DNA-binding protein. J. Bacteriol. **188:**6153–6167.
24. **Matsumiya, S., S. Ishino, Y. Ishino, and K. Morikawa.** 2002. Physical interaction between proliferating cell nuclear antigen and replication factor C from *Pyrococcus furiosus*. Genes Cells **7:**911–922.
25. **Mayanagi, K., T. Miyata, T. Oyama, Y. Ishino, and K. Morikawa.** 2001. Three-dimensional electron microscopy of the clamp loader small subunit from *Pyrococcus furiosus*. J. Struct. Biol. **134:**35–45.
26. **Nishida, H., S. Ishino, T. Miyata, K. Morikawa, and Y. Morikawa.** 2005. Identification of the critical region in replication factor C from *Pyrococcus furiosus* for the stable complex formation with proliferating cell nuclear antigen and DNA. Genes Genet. Syst. **80:**83–93.
27. **Oyama, T., Y. Ishino, I. K. Cann, S. Ishino, and K. Morikawa.** 2001. Atomic structure of the clamp loader small subunit from *Pyrococcus furiosus*. Mol. Cell **8:**455–463.
28. **Pan, Z. Q., M. Chen, and J. Hurwitz.** 1993. The subunits of activator 1 (replication factor C) carry out multiple functions essential for proliferating-cell nuclear antigen-dependent DNA synthesis. Proc. Natl. Acad. Sci. USA **90:**6–10.
29. **Pisani, F. M., M. De Felice, F. Carpentieri, and M. Rossi.** 2000. Biochemical characterization of a clamp-loader complex homologous to eukaryotic replication factor C from the hyperthermophilic archaeon *Sulfolobus solfataricus*. J. Mol. Biol. **301:**61–73.
30. **Robbins, J. B., M. C. McKinney, C. E. Guzman, B. Sriratana, S. Fitz-Gibbon, T. Ha, and I. K. Cann.** 2005. The Euryarchaeota: nature's medium for engineering of single-stranded DNA binding proteins. J. Biol. Chem. **280:**15325–15339.
31. **Seybert, A., D. J. Scott, S. Scaife, M. R. Singleton, and D. B. Wigley.** 2002. Biochemical characterisation of the clamp/clamp loader proteins from the euryarchaeon *Archaeoglobus fulgidus*. Nucleic Acids Res. **30:**4329–4338.
32. **Seybert, A., M. R. Singleton, N. Cook, D. R. Hall, and D. B. Wigley.** 2006. Communication between subunits within an archaeal clamp-loader complex. EMBO J. **25:**2209–2218.
33. **Turner, J., M. M. Hingorani, Z. Kelman, and M. O'Donnell.** 1999. The internal workings of a DNA polymerase clamp-loading machine. EMBO J. **18:**771–783.
34. **Warbrick, E.** 1998. PCNA binding through a conserved motif. Bioessays **20:**195–199.
35. **Yao, N., L. Coryell, D. Zhang, R. E. Georgescu, J. Finkelstein, M. M. Coman, M. M. Hingorani, and M. O'Donnell.** 2003. Replication factor C clamp loader subunit arrangement within the circular pentamer and its attachment points to proliferating cell nuclear antigen. J. Biol. Chem. **278:**50744–50753.
36. **Zhuang, Z., B. L. Yoder, P. M. Burgers, and S. J. Benkovic.** 2006. The structure of a ring-opened proliferating cell nuclear antigen-replication factor C complex revealed by fluorescence energy transfer. Proc. Natl. Acad. Sci. USA **103:**2546–2551.